Results & Discussion

Role of Poly {ADP-Ribose} Polymerase (PARP) in UV-C induced cell death in *D. discoideum*

3.1. Introduction

Radiation and chemical mutagens are direct DNA damaging agents. Ultra Violet (UV) radiation, that comprises a broad band of energy extending from 200 to 400 nm, is one of the frequently used radiations in biological studies. The UV part of the solar electromagnetic spectrum can be subdivided into three regions: UV-C (200-280 nm), UV-B (280-315 nm) and UV-A (315-400 nm). UV-B radiation is the main waveband responsible for sunburn, skin aging and skin cancer induction. UV-A is carcinogenic and less biologically active than UV-B. UV-C is the most harmful UV radiation and nonetheless it does not reach the earth due to ozone layer. However, consequent to ozone depletion, UV-C could become the biggest challenge to be encountered by living organisms in near future. All cellular constituents can absorb UV-C radiation and subsequently free radicals could be produced in cells (Denecker *et al.*, 2001). While oxidative stress induced by ionizing radiation and alkylating agents accounts for the DNA damage induced by these agents, ROS are not the major cause of DNA damage in UV-C irradiated cells.

UV-C can cause formation of thymine glycol (Dimple and Linn, 1982) and pyrimidine hydrates (Boorstein *et al.*, 1990). However the main lesions are cyclobutane pyrimidine dimers and pyrimidine-(6-4)-pyrimidone photoproducts (Gentill *et al.*, 1997). More than half of the cyclobutane pyrimidine dimers occur in thymine-thymine (T-T) doublets and in cytosine-thymine (C-T) doublets (Tornaletti *et al.*, 1993). Pyrimidine-(6-4)-pyrimidone photoproducts are formed by a stable bond between positions 6 and 4 preferentially of a T-C doublet followed by C-C and T-T doublets. In double stranded DNA these lesions are formed in a ration of 3:1 (Aboussekhra and Wood, 1994) and lead to generation of SSBs (Single strand breaks) when they are repaired by the NER (Nucleotide excision repair system) (Friedberg 1996). Both types of lesions lead to distortion in DNA double helical structure which is sufficient to activate PARP, a nuclear enzyme that is known to get activated due to DNA damage (Rouleau *et al.*, 2004). PARP catalyses PARylation of various proteins along with its own modification. Different PARP substrates are involved in a wide range of physiological processes. Our interest is

to study the role of PARP in UV-C induced cell death mechanism in *D. discoideum*, a model organism that lacks caspases.

3.2. Results

3.2.1 Induction of cell death in *D. discoideum* cells by UV-C irradiation and the delay induced by PARP inhibition

Experiments were designed to establish the ability of *D. discoideum* to undertake cell death after UV-C exposure. *D. discoideum* cells were subjected to different doses of UV-C irradiation (0-130 J/m^2) and cell death was monitored by trypan blue exclusion method and Annexin V staining at different post irradiation periods (1-22 hours) and the results are shown in Figures 3.1 and 3.2.

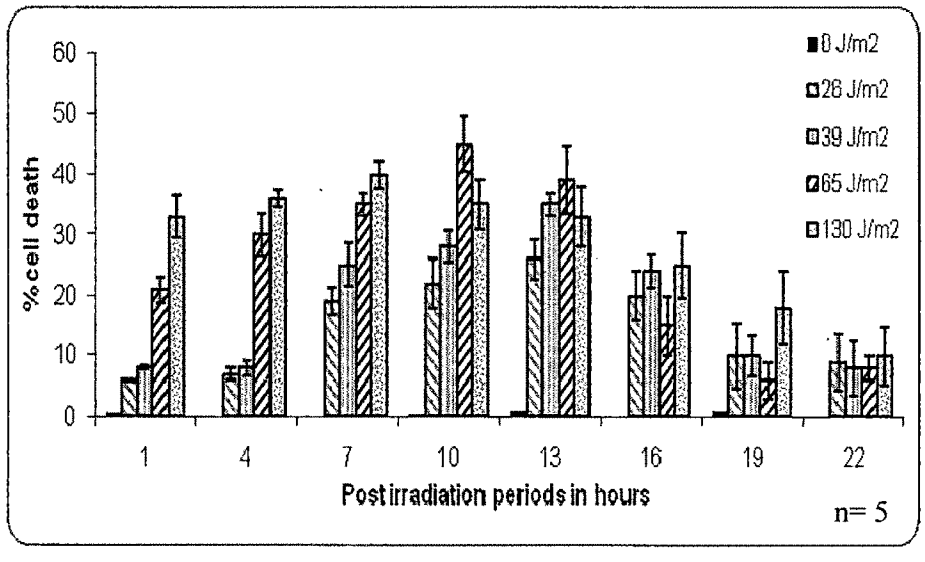

Figure 3.1: UV-C induced dose dependent cell death as monitored by trypan blue exclusion method. Data (mean ± S.E.) are from five independent experiments.

Early cell death was observed at 65 J/m^2 and 130 J/m^2 UV-C treated cells whereas, with 26 J/m^2 and 39 J/m^2 UV-C treatment, percent cell death in early phase was less and it increased after 7 hours (Fig. 3.1). These results suggest 65 J/m^2 and 130 J/m^2 UV-C doses to be necrotic, whereas 26 J/m^2 and 39 J/m^2 UV-C doses to be paraptotic for *D. discoideum* cells.

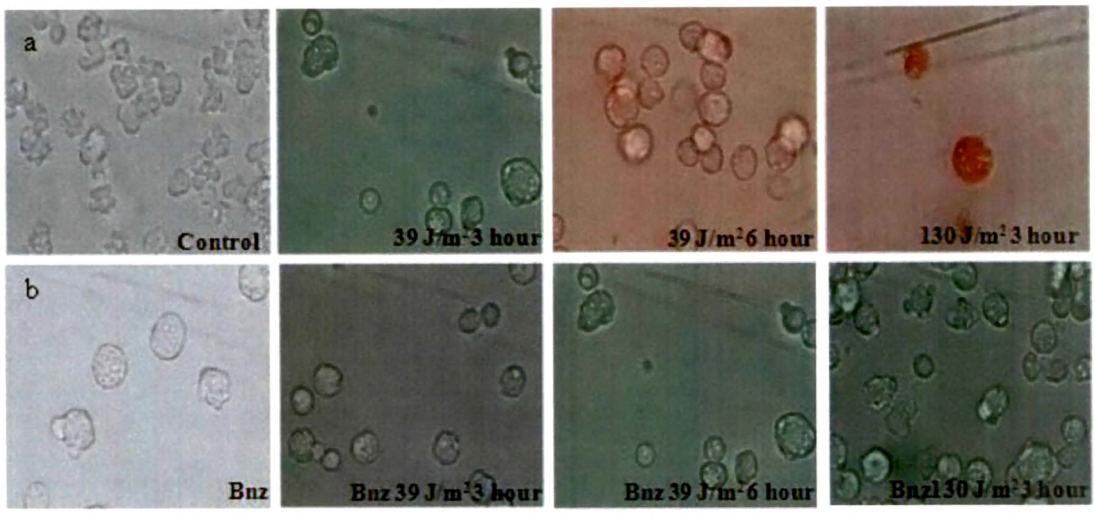

Figure 3.2: Annexin V staining of UV-C irradiated *D. discoideum* cells. a) PS exposure is seen at 3 hours while PI staining at 6 hours with 39 J/m^2. 130 J/m^2 was found to be necrotic as both AnnexinV-FITC and PI staining were observed at 3 hours. b) Effect of benzamide pretreatment on UV-C induced cell death. Data are representative of at least three independent experiments. Photographs were taken with 60X objective.

As can be seen from Figure 3.2, cells were PS positive and PI negative 3 hours after 39 J/m^2 UV-C exposure; however after 6 hours irradiated cells were PS as well as PI positive. Thus PS-PI dual staining results confirmed 39 J/m^2 UV-C dose to be paraptotic for *D. discoideum* cells. Unlike 39 J/m^2, 130 J/m^2 UV-C treated cells were PS and PI positive 3 hours after stress thereby confirming 130 J/m^2 UV-C dose to be necrotic for *D. discoideum* cells. Thus the paraptotic and necrotic doses of UV-C for *D. discoideum* cells by PS-PI dual staining were confirmed.

Pretreatment of cells with PARP inhibitor- benzamide prior to irradiation showed delay in cell death induced by UV-C as shown in the Figure 3.2 130 J/m^2 UV-C irradiation led to paraptosis in the presence of benzamide instead of necrosis; also 39 J/m^2 UV-C irradiation with benzamide pretreatment led to paraptosis that was delayed by 2 hours. This showed the involvement of PARP in UV-C induced cell death.

3.2.2 PARP activation and its inhibition by benzamide under UV-C stress

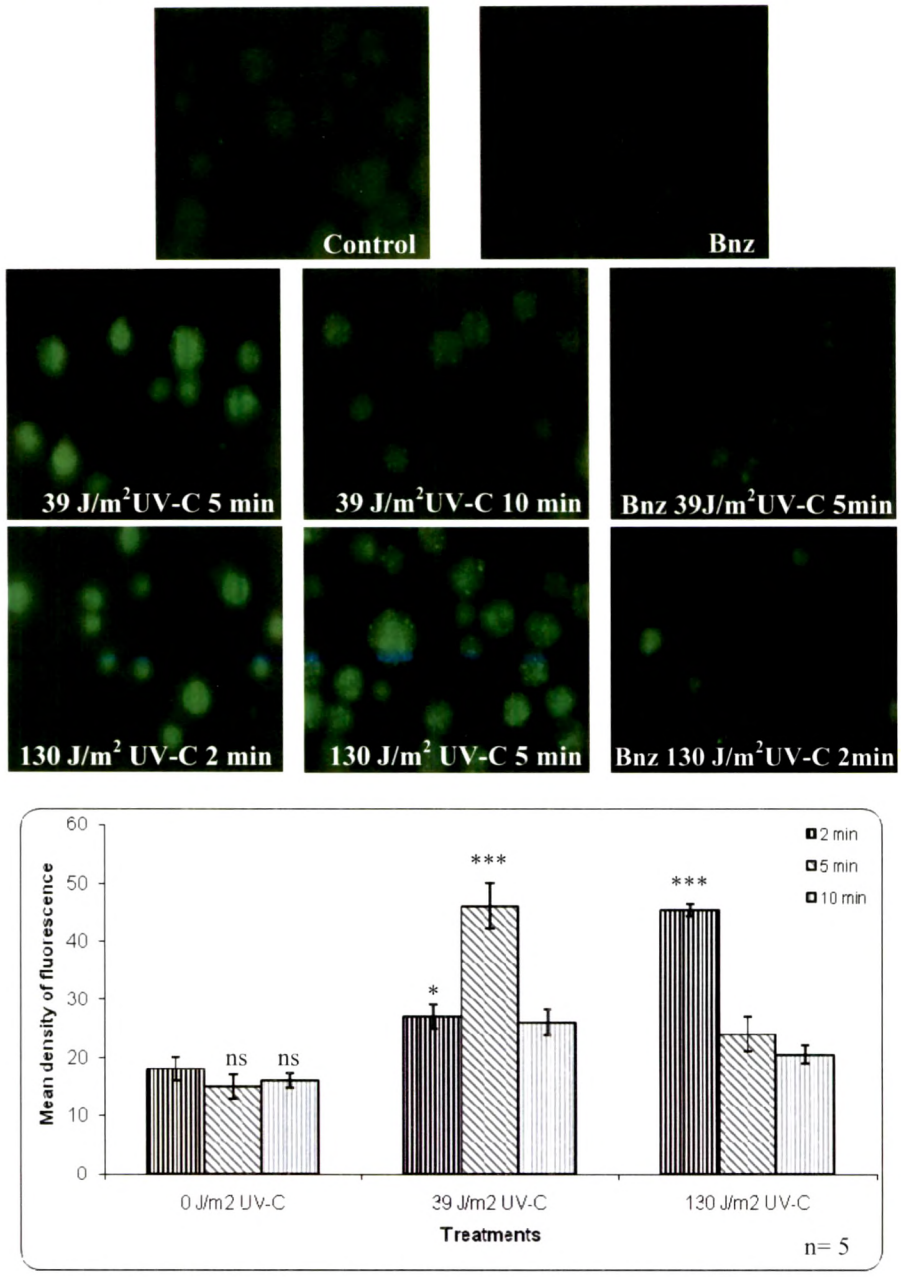

Figure 3.3a and b: PARP activity assay by indirect immunofluorescence. PARP activity was measured at different time points post UV-C irradiation. a) Photographs were taken with 60X objective. b) Densitometric analysis of PARP activity. Under control conditions basal PARP activity was observed. Peak activity of PARP was seen at 5 minutes post 39 J/m^2 UV-C irradiation which reached basal level within 15 minutes. Cells when treated with 130 J/m^2 UV-C showed increased PAR immunoreactivity at 2 minutes. Data (mean ± S.E.) are from five independent experiments. ns (non significant), * p value <0.05 compared to control.*** p value <0.001 compared to control.

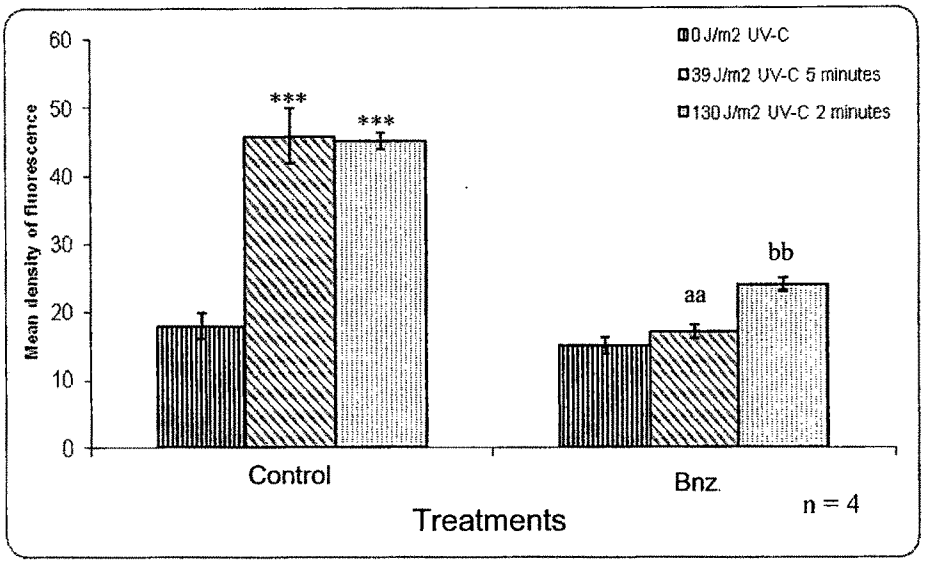

Figure 3.3c: Peak PARP activity induced by UV-C irradiation was intercepted by benzamide. Benzamide inhibited PARP activity at 5 minutes and 2 minutes post 39 J/m^2 and 130 J/m^2 irradiation respectively. Data (mean ± S.E.) are from four independent experiments. *** p value <0.001 as compared to control; $^{aa, bb}$ p value <0.01compared to 39 J/m^2 and 130 J/m^2 respectively.

To study the kinetics of PARP activation PARP activity was assayed at various time points (2, 5, 10 and 15 minutes) post UV-C irradiation and the results are shown in Figures 3.3a and b. Also shown in the Figures 3.3a and c is that PARP activation could be prevented using benzamide. Peak PARP activity was observed 5 minutes after 39 J/m^2 UV-C irradiation which then declined, and reached to basal level by 15 minutes (Fig. 3.3 a and b). Benzamide pretreated cells did not show activation of PARP after 39 J/m^2 UV-C treatment (Fig. 3.3a and c). 130J/m^2 UV-C irradiated cells showed a peak in PARP activity after 2 minutes which then declined and reached to basal levels by 10 minutes (Fig. 3.3 a and b). Benzamide pretreated cells showed significant inhibition in the PARP activity (Fig. 3.3 a and c).

3.2.3. PARP activation leads to adenine and pyridine nucleotides depletion

Consequent to PARP activation cellular NAD^+ as well as ATP pools deplete, later as a result of cellular attempt to replenish the reduced NAD^+ levels of the cells. Depleted adenine nucleotides are one of the probable candidate signals responsible for the downstream events in the paraptotic pathway. NAD^+ and ATP levels were monitored in

control and UV-C irradiated cells and the results are shown in Figures 3.4 and 3.5. NAD^+ and ATP contents were reduced to ~50% and 55% of control values respectively within 1 hour of 39 J/m^2 exposure (Fig. 3.4 and 3.5). Additionally, 130 J/m^2 irradiated *D. discoideum* cells also exhibited a sharp decline (~80 and 75% reduction respectively) in NAD^+ and ATP levels within 1 hour of irradiation (Fig. 3.4 and 3.5). These results support the early activation of PARP.

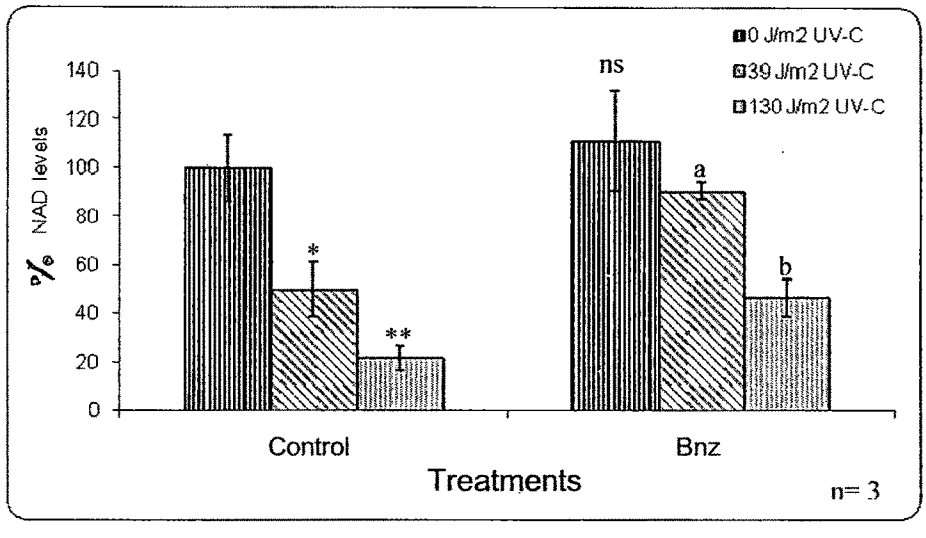

Figure 3.4: UV-C irradiation depletes NAD^+ content of *D. discoideum* cells in an hour in a PARP dependent manner. Data (mean ± S.E.) are from three independent experiments. ns (non significant), * p value <0.05 and ** p value <0.01 compared to control; [a, b] p value <0.05 compared to respective UV-C dose.

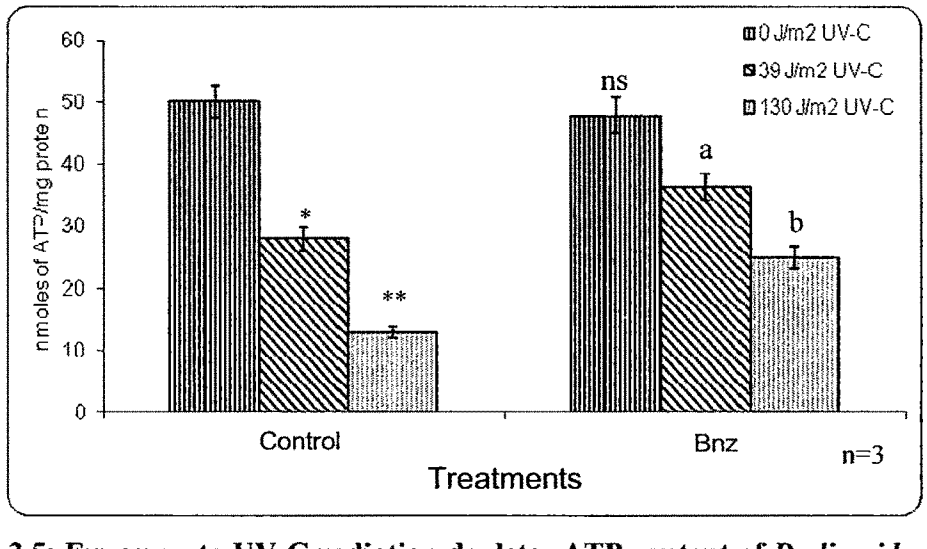

Figure 3.5: Exposure to UV-C radiation depletes ATP content of *D. discoideum* cells in a PARP dependent manner within 1 hour. Data (mean ± S.E.) are from three independent experiments. ns (non significant), * p value <0.05 and ** p value <0.01 compared to control; [a, b] p value <0.05 compared to respective UV-C dose.

PARP inhibition studies with benzamide showed significant restoration of cellular NAD^+ and ATP levels. NAD^+ and ATP levels were restored by 40% and 15% respectively in 39 J/m^2 irradiated *D. discoideum* cells. During necrosis (130 J/m^2) PARP inhibition showed ~25 % rescue in both NAD^+ and ATP levels (Fig. 3.4 and 3.5), indicating that PARP activation caused reduction in cellular energy levels.

3.2.4 MMP changes after UV-C exposure in context to PARP activation

Change in mitochondrial membrane potential is one of the key events during cell death. In order to determine the involvement of PARP in UV-C induced cell death changes in MMP using the membrane potential sensitive dye $DiOC_6$ were examined in the presence and absence of benzamide.

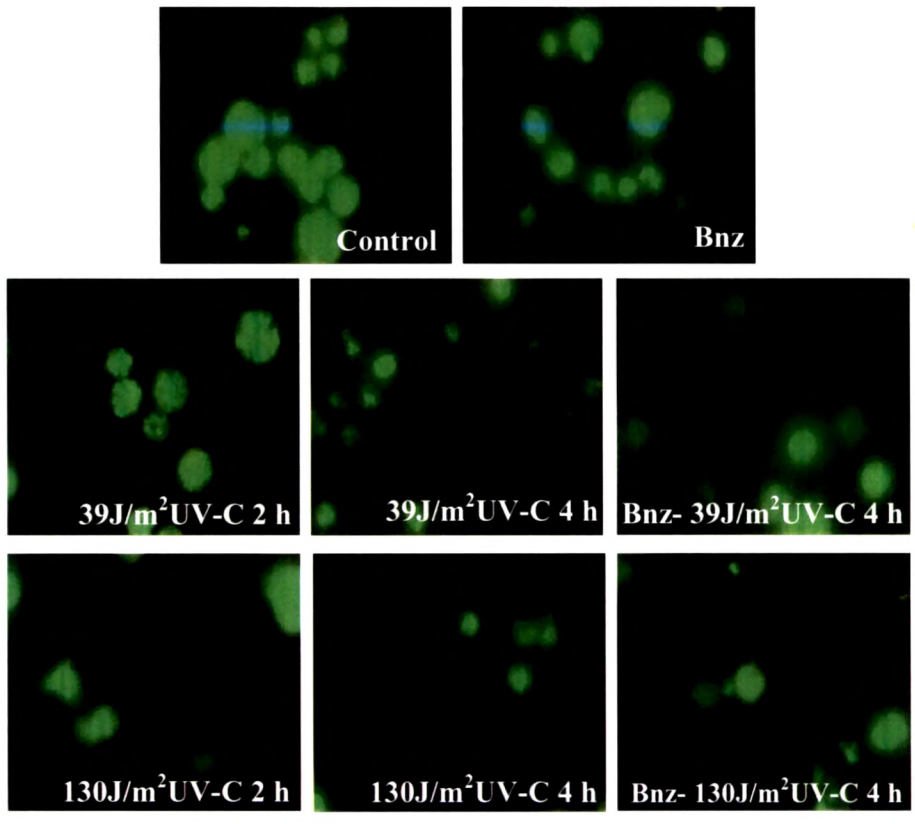

Figure 3.6a: Mitochondrial membrane potential changes induced by UV-C irradiation. Live cells accumulate the dye in mitochondria hence fluorescence intensity was found to be high in control and decreased with UV-C stress. Benzamide partially restored the changes in MMP. Data are representative of at least five independent experiments. Photographs were taken with 60X objective.

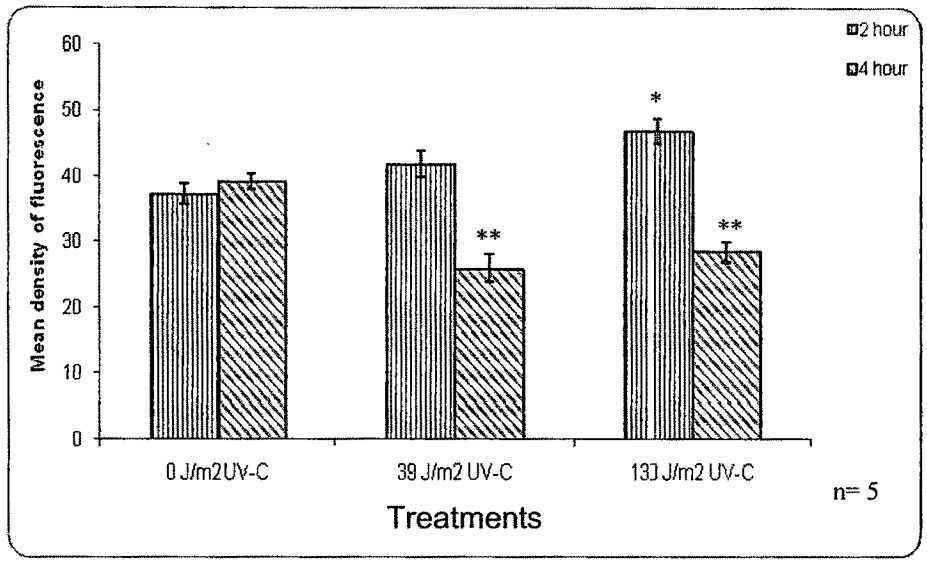

Figure 3.6b: Densitometric analysis of time dependent changes in mitochondrial membrane potential after UV-C irradiation. Significant increase was found at 2 hours with necrotic dose. MMP decreased significantly in both paraptotic and necrotic cell 4 hours after UV-C irradiation. Data (mean ± S.E.) are from five independent experiments. ** p value <0.01, * p value <0.05 compared to control.

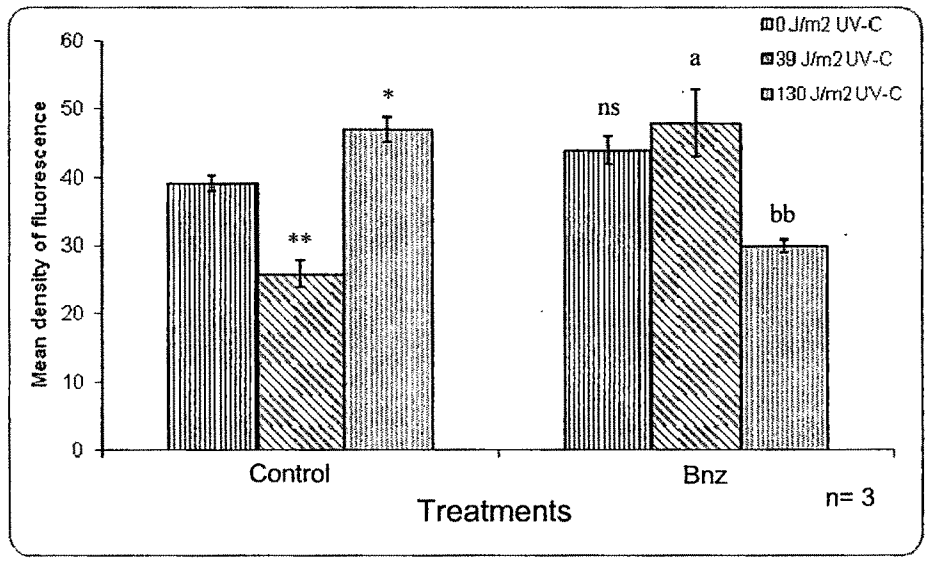

Figure 3.6c: Mitochondrial membrane potential changes induced by UV-C irradiation were partially rescued by benzamide. MMP change with 39 J/m^2 at 4 hours and 130 J/m^2 UV-C at 2 hours was partially restored by benzamide. Data (mean ± S.E.) are from three independent experiments. ** p value <0.01, compared to control; ^{a} p value <0.05 compared to 39 J/m^2; ^{bb} p value <0.01 compared to 130 J/m^2.

Paraptotic dose led to rise in MMP, although non significant, at an early stage (Fig. 3.6 a and b). Nevertheless significant increase was observed in mitochondrial membrane potential in the initial phase of necrotic death (Fig. 3.6 a and b). Significant reduction in MMP was observed later during the course of cell death i.e. 4 hours after irradiation with 39 J/m^2 as well as 130 J/m^2 doses of UV-C (Fig. 3.6 a and b). Benzamide pretreatment partially restored MMP in cells irradiated with UV-C (Fig. 3.6 a and c), nonetheless the rescuing effect on MMP changes induced by necrotic dose is less (Fig. 3.6 a and c). These results are in agreement with nucleotide depletion results.

3.2.5. AIF translocation is downstream to PARP activation

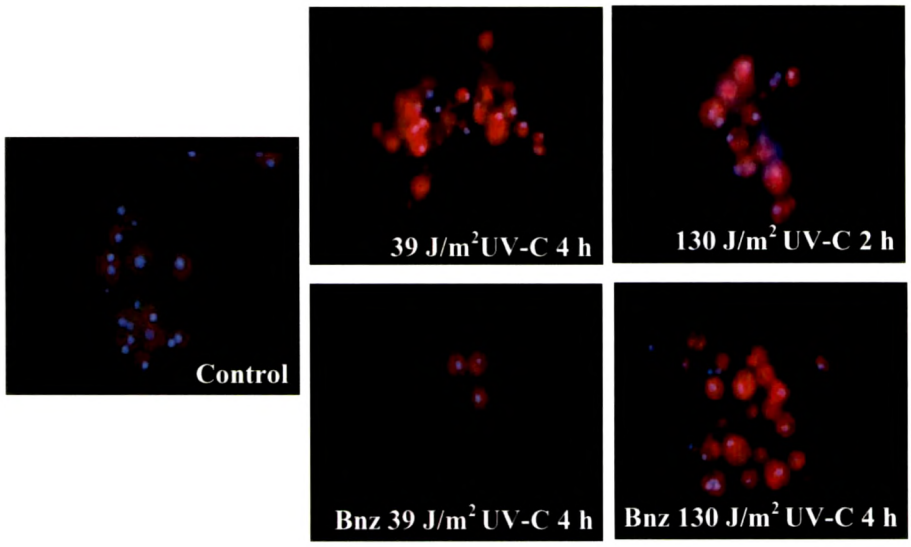

Figure 3.7: Fluorescence microscopy for the mitochondria-nuclear translocation of AIF after exposure to different doses of UV-C at different time points in the presence and absence of benzamide. Data are representative of at least five independent experiments. Photographs were taken with 60X objective.

Apoptosis inducing factor (AIF) translocation has been identified as a mediator of PARP induced cell death. During UV-C induced cell death AIF release was observed at different time points with paraptotic and necrotic doses. With 39 J/m^2 UV-C exposure translocation was seen at 4 hours (Fig. 3.7). These changes in the localization of AIF coincide with the MMP changes. During necrosis i.e., with 130 J/m^2 UV-C AIF release was seen by 2 hours (Fig. 3.7) along with MMP change. Inhibition of PARP activity by benzamide intercepted

this AIF release during paraptosis however, with 130 J/m^2 UV-C irradiation benzamide pretreatment did not affect AIF nuclear translocation (Fig. 3.7).

3.2.6. Monitoring the release of cytochrome c from mitochondria

As *D. discoideum* exhibits caspase independent cell death, release of cytochrome c from mitochondria may not be of much significance. However we have observed the release of cytochrome c at 2 hours during *D. discoideum* paraptotic cell death (Fig. 3.8). Thus cytochrome c release could affect the functioning of mitochondria as it coincides with MMP changes and is upstream to mitochondrial AIF release and further its translocation to the nucleus.

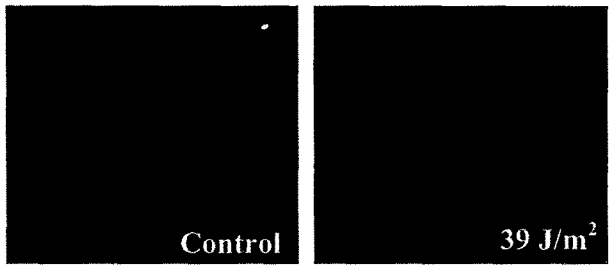

Figure 3.8: Cytochrome c release during paraptosis by immunofluorescence. Punctate staining in control cells indicate the localization of cyt c in mitochondria while diffused staining with UV-C treatment indicate release of cytochrome c into cytosol at 2 hours. Data are representative of three independent experiments. Photographs were taken with 60X objective.

3.2.7. UV-C induced paraptosis leads to large scale DNA fragmentation

Oligonucleosomal DNA fragmentation is hallmark of apoptosis while paraptosis exhibits large scale DNA fragmentation. Such fragments cannot be resolved on agarose gel. DNA of *D. discoideum* cells exposed to 39 J/m^2 UV-C when subjected to agarose gel electrophoresis showed absence of oligonucleosomal DNA ladder (Fig. 3.9). DNA fragmentation could be detected by TUNEL assay and a significant increase in TUNEL positive cells was seen (Figs. 3.10 a and b) at 6 hours post 39 J/m^2 UV-C stress suggesting that *D. discoideum* cells undergo large scale DNA fragmentation. However, 130 J/m^2 UV-C irradiated cells exhibited DNA smear on agarose gel electrophoresis (Fig. 3.9) supporting the cell death to be of necrotic type. Thus these results reinforce that *D. discoideum* exhibits PARP mediated paraptosis and necrosis under low and high levels of UV-C stress respectively.

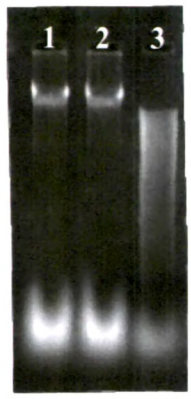

Figure 3.9: Monitoring DNA Fragmentation by agarose gel electrophoresis.

Lane 1: DNA from control cell

Lane 2: DNA from 39 J/m^2 UV-C irradiated cells

Lane 3: DNA from 130 J/m^2 UV-C irradiated cells

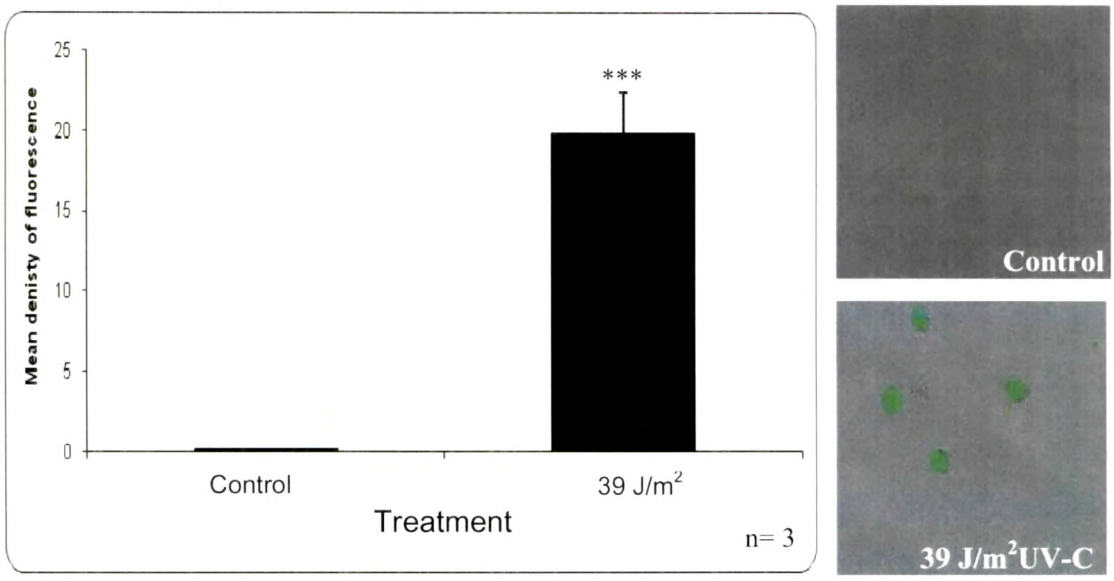

Figure 3.10: DNA fragmentation under UV-C stress was monitored using TUNEL assay. Photographs were taken under 60X objective. Densitometric analysis of DNA fragmentation. Data (mean ± S.E.) are from three independent experiments. *** p value <0.001 compared to control.

3.2.8. Characterization of paraptotic vesicles

As a consequence to PCD cells form vesicles. Formation of vesicles at later stage of UV-C induced cell death after loss of plasma membrane integrity was studied. Our results on biochemical characterization of the paraptotic vesicles formed under UV-C induced paraptotic cell death (39 J/m^2 UV-C exposure) in *D. discoideum* suggest that the vesicles were membranous in nature (Fig. 3.11a) and contain DNA (Fig. 3.11b). No such vesicles were observed with necrotic cells.

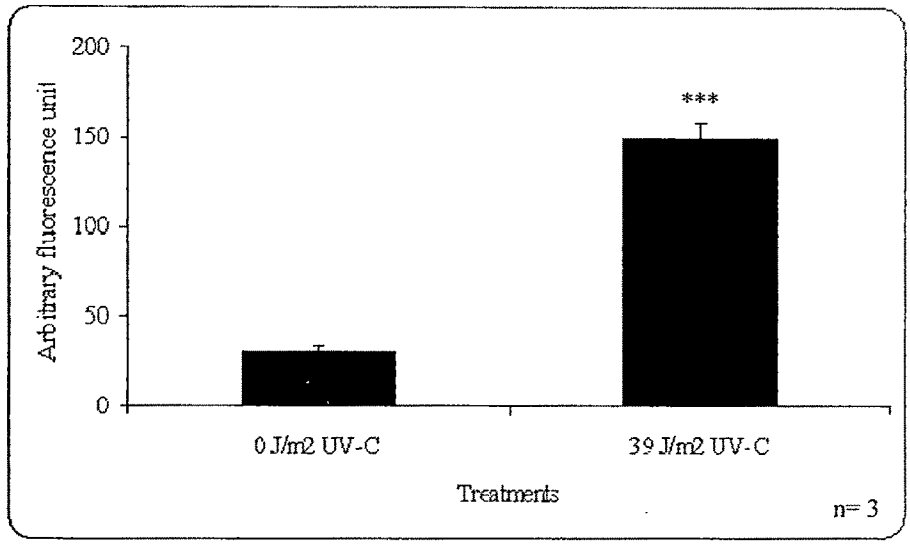

Figure 3.11a: Characterization of paraptotic vesicles formed during UV-C stress using membrane probe DPH by fluorimetry. Data (mean ± S.E.) are from three independent experiments. *** p value <0.001 compared to control.

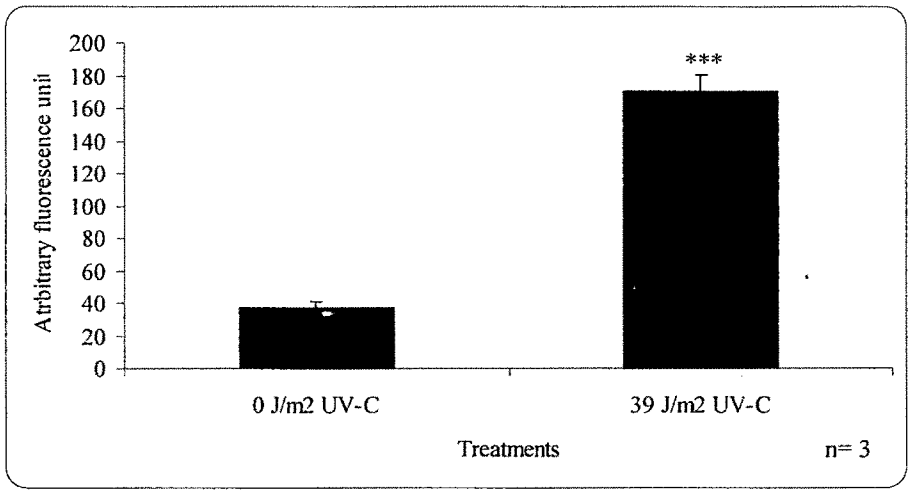

Figure 3.11b: Characterization of paraptotic vesicles formed during UV-C stress using DNA binding dye DAPI. Data (mean ± S.E.) are from three independent experiments. *** p value <0.001 compared to control.

3.2.9. Effect of broad caspase inhibitor on UV-C induced cell death

To demonstrate that the cytotoxicity effect is not due to caspase dependent pathway, cell death study was carried out with broad caspase inhibitor (zVAD-fmk). In the presence of 10 μM zVAD-fmk, the cytotoxicity induced by UV-C stress was not inhibited indicating that *D. discoideum* cells take up caspase independent pathway. Further increasing the concentration of zVAD-fmk up to 25 μM did not change our results (Fig. 3.12).

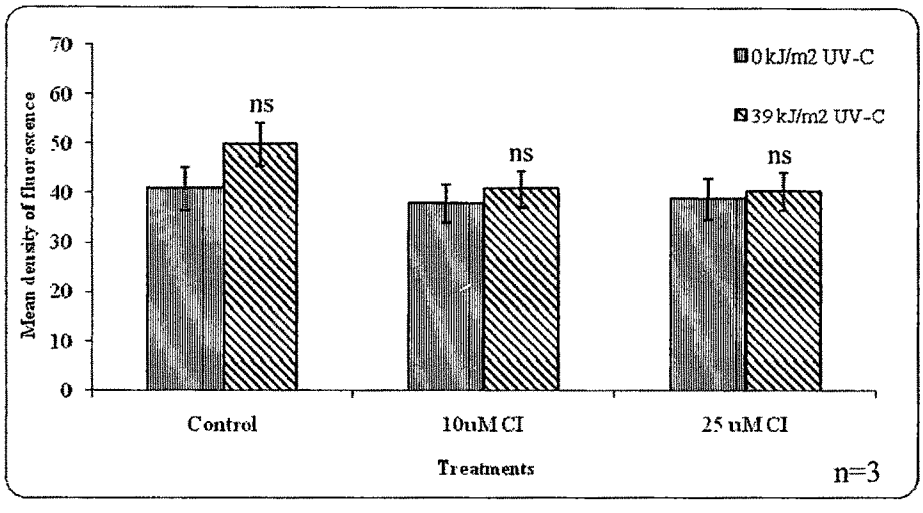

Figure 3.12: Caspase activity during paraptotic cell death. *D. discoideum* cells were irradiated with UV-C and caspase activity was assayed at 6 hours in form of DEVD-AMC cleavage and also in presence of caspase inhibitor (CI). Data (mean ± S.E.) are from three independent experiments. Caspase activity was non significant.

3.2.10. Effect of MEK inhibition on cell death

A recent report suggests the involvement of MEK (mitogen-activated protein kinase kinase) signaling in paraptosis (Sperandio *et al.*, 2004). To study the involvement of MEK in UV-C induced cell death studies were done using two different doses of MEK inhibitor i.e., U0126 (1,4-diamino-2,3-dicyano-1,4-bis[2-aminophenylthio] butadiene) which has been shown to be a highly selective inhibitor of MEK 1 and MEK 2 . MEK inhibition could not rescue UV-C induced cell death (Fig. 3.13).

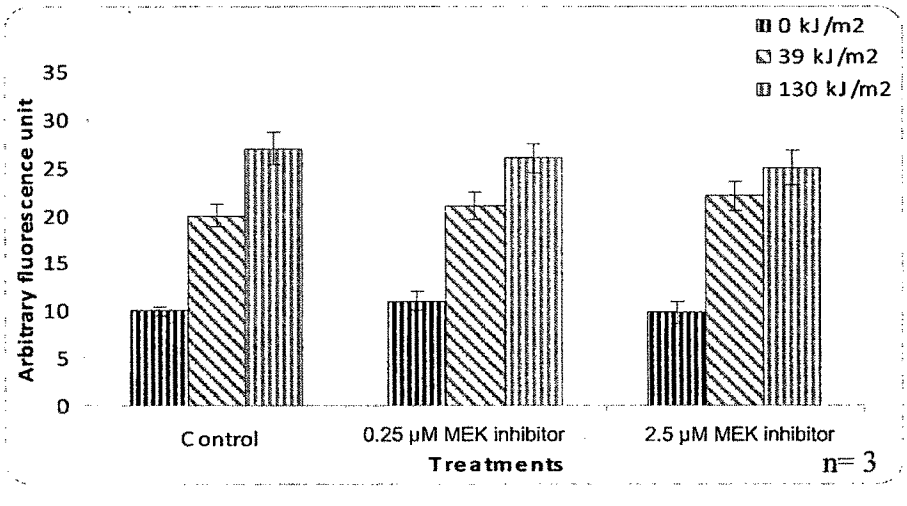

Figure 3.13: Propidium iodide staining to observe cell death upon MEK inhibition. Data (mean ± S.E.) are from three independent experiments. MEK inhibition did not show significant change in PI staining.

3.3 Discussion

3.3.1. Cell death characterization

UV-C is one of the most harmful radiations and we have studied the effect of UV-C on *D. discoideum*, which is known to exhibit high resistance to different DNA damaging agents (Deering, 1988). Our studies on 65 and 130 J/m^2 doses of UV-C irradiation, as monitored with trypan blue assay, showed death of cells in the early hours i.e. within 1-4 hours which was more likely to be necrotic type of cell death, whereas with 26 and 39 J/m^2 doses cell death occurred at or after 7 hours which was of paraptotic type. Our PS-PI dual staining results with 39 and 130 J/m^2 UV-C exposed cells confirmed that 39 J/m^2 UV-C dose is paraptotic while 130 J/m^2 dose is necrotic (Fig. 3.2).

3.3.2. UV-C irradiation and PARP activation

Eukaryotic cells have nuclear enzyme poly(ADP-ribose) polymerase (PARP) that gets activated in response to DNA damage by different chemical and physical agents (Burkle *et al.*, 2000), including UV-C (230-280 nm). Also many characteristics of this enzyme make it an ideal candidate for participation in cellular responses to UV stress (Jacobson *et al.*, 2001). Several earlier studies focused on examining activation of PARP in UV-C irradiated cells, and these reports suggest that PARP is activated when DNA strand breaks are generated during excision repair (Alvarez-Gonzalez and Althaus, 1989; Berger *et al.*, 1980; McCurry and Jacobson, 1981; Yoon *et al.*, 1996). UV-C induces direct DNA lesions such as other CPDs (e.g. T-T, T-C or C-C) or 6,4-photoproducts. These can serve to attract and activate PARP as all of these lesions distort DNA structure and it is likely that PARP can recognize and bind to this unusual DNA structure. Using elegant techniques that allow visualization of events occurring in UV-C irradiated zone Vodenicharov *et al* (2005) have shown that the cause of immediate PARP activation within the first 15 seconds to 5 minutes after UV-C irradiation is direct DNA damage. In our studies *D. discoideum* cells subjected to paraptotic dose of UV-C i.e. 39 J/m^2 exhibit activation of PARP in 5 minutes that declines to basal levels by 15 minutes (Fig. 3.3 a and b). Necrotic dose (130 J/m^2) led to faster activation of PARP within 2 minutes and activity later declined to basal levels by 10 minutes (Fig. 3.3 a and b). This pattern of PARP activity matches with that demonstrated in mouse embryonic fibroblast cells subjected to UV-C (Vodenicharov *et al.*, 2005). HeLa cells when subjected to MNNG

stress, a DNA alkylating agent, also showed peak PARP activity at ~5 minutes (Cipriani *et al.*, 2005).

PARP activation is a dynamic and flexible metabolism that can be targeted to the site of specific DNA damage at a desired time to participate in a specific response of higher eukaryotic cells to DNA damage (Vodenicharov *et al.*, 2005). There are many possible functions for the immediate activation of PARP at the site of direct DNA damage by UV-B or UV-C. More specifically, in response to UV, PARP activation has been shown to participate in carcinogenesis, DNA repair and cell death. Early and rapid PARP activation in cells exposed to high levels of DNA damage by alkylating agents has been associated with subsequent apoptotic or necrotic death (Hong *et al.*, 2004; Zong *et al.*, 2004).

3.3.3. Immediate consequences of PARP activation during paraptotic and necrotic cell death

Peak PARP activity was observed 5 minutes after 39 J/m^2 irradiation and at 2 minutes after 130 J/m^2 irradiation in *D. discoideum* (Fig. 3.3 a and b). Pretreatment with benzamide resulted in inhibition of increased PARP activity at both the doses of UV-C (Fig. 3.3 a and c).

In general, it is known that activated PARP utilizes nicotinamide-adenine dinucleotide (NAD^+) to form polymers of ADP-ribose (pADPr) on itself and a few selected DNA metabolism-related proteins. Subsequent to PARP activation NAD^+ levels get depleted, and ATP is required for NAD^+ replenishment (Kim *et al.*, 1994) hence PARP activation causes reduction in cellular energy levels. Benzamide pretreatment results confirm that at paraptotic and necrotic (39 J/m^2 and 130 J/m^2) doses *D. discoideum* cells experience reduction in NAD^+ and hence in the ATP levels in a PARP dependent manner (Figs. 3.4 and 3.5).

Poly ADP ribosylation is a post-translational modification that transiently alters normal functions of substrate proteins until they are restored to their native state by removal of pADPr chains. Thus Poly ADP ribosylation, NAD^+ and ATP depletion and modification of various proteins are the consequences of PARP activation which could independently or in combination lead to further downstream events of PARP mediated cell death.

3.3.4. Late consequences of PARP activation during paraptotic and necrotic cell death

PARP activation during peroxynitrite and hydrogen peroxide stress conditions is responsible for the loss of MMP since the reduction in MMP is blocked by inhibiting PARP. In this study both doses of UV-C (39 and 130 J/m^2) lead to early PARP activation and NAD^+ and ATP depletion followed by reduction in MMP by 4 hours (Fig. 3.6 a and b) (the mmp changes start at 2 hours itself though the change is not significant) and PS exposure at 3 hours (Fig. 3.2) after irradiation. These changes are dependent on activation of PARP since inhibition of PARP activity with benzamide led to partial restoration of MMP and also delayed PS exposure by 2 hours (Fig. 3.6 a, b and 3.2). Zamzami *et al* (1995) demonstrated reduction in MMP in peripheral lymphocytes treated with dexamethasone or SEB (*Staphylococcus aureus* enterotoxin B) to be a committed step for PCD. These changes are followed by other PCD-associated changes such as DNA fragmentation and loss of plasma membrane integrity as measured by PI staining.

Reduction in MMP is linked to mitochondrial outer membrane permeabilisation which leads to the release of proapoptotic proteins like AIF into the cytosol to carry forward the execution of PARP triggered cell death (Modjtahedi *et al*., 2006). In the present study AIF is shown to be released at 4 and 2 hours after exposure to paraptotic and necrotic doses (39 and 130 J/m^2) of UV-C respectively (Fig. 3.7). While other studies focus on the caspase dependent machinery of cell death, however ours is one of the few studies that report release of AIF from mitochondria following exposure to UV-C. Chopra *et al* (2009) have reported the release of AIF from mitochondria following UV irradiation. This release of AIF from mitochondria after UV-C exposure is again a PARP dependent event. Translocated AIF in the nucleus is known to interact with cyclophilin A forming an active DNase to carry out the characteristic large scale DNA fragmentation during paraptosis (Modjtahedi *et al*., 2006). *D. discoideum* cells exposed to UV-C also exhibit large scale DNA fragmentation downstream to AIF translocation (Fig. 3.9, 3.10 a and b).

Apoptotic vesicle formation is a characteristic feature of programmed cell death. *D. discoideum* cells undergo paraptotic cell death in conditioned medium with the release of apoptotic vesicle like bodies characterized by the presence of DNA, protoporphyrin IX and phosphatidyl serine exposure (Arnoult *et al*., 2001). Interestingly, *D. discoideum* exhibited paraptotic vesicle formation during UV-C induced paraptotic cell death. These vesicles consisted of DNA surrounded by a membrane as they were stained with DPH and

DAPI (Fig. 3.11 a and b) but did not contain protoporphyrin IX. However, vesicles were not detected during necrotic cell death.

3.3.5. Role of caspases and MEK during PARP initiated cell death

Caspase is the most extensively studied downstream executioner of programmed cell death. Programmed cell death and caspases have been considered to go hand in hand until recently. However, PARP mediated cell death is a mushrooming aspect of cell death studies which is devoid of the contribution of caspases (Hong *et al.*, 2004). Predictably no effect was observed on UV-C induced paraptosis in *D. discoideum* cells with broad caspase inhibitors (Fig. 3.12).

The role of MEK (mitogen-activated protein kinase kinase) in UV-C induced tumor progression has been addressed (Shaw *et al.*, 2004). Involvement of MEK during oxidative stress induced cell death in various mammalian cell lines namely human neuroblastoma SH-SY5Y cells (Saeki *et al.*, 2000) is well known. However, involvement of MEK in UV-C induced paraptosis has not been addressed. Results presented in this study show that MEK does not have a role in PARP mediated paraptotic cell death induced by UV-C (Fig. 3.13).

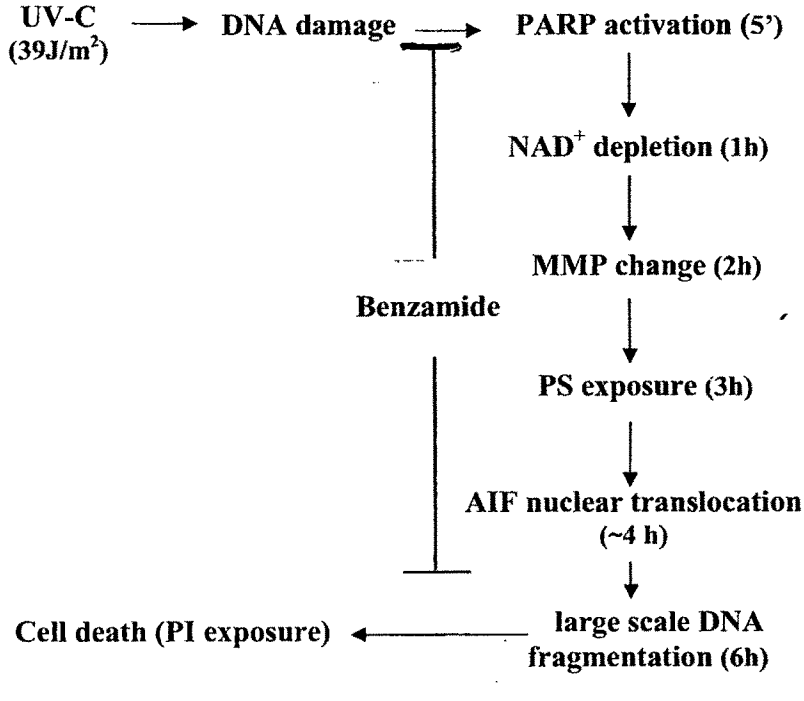

Figure 1.14: Proposed pathway for UV-C induced cell death in *D. discoideum*

The present study provides the facts pertaining to involvement of PARP and the kinetics of events during UV-C induced cell death in *D. discoideum*. Energy derangement, mitochondrial changes, AIF translocation, and DNA fragmentation occur in sequence during UV-C induced paraptosis in a PARP dependent manner as par with mammalian systems (Fig. 1.14) (Zhang *et al.*, 1994; Endress *et al.*, 1997). Paraptotic cell death in *D. discoideum* shows conservation of the necessary machinery as mammalian systems hence these studies can be extrapolated to higher eukaryotes.

It has been reported that paraptosis also can be seen in mammalian cells. Interestingly mammalian paraptosis is mediated by procaspase-9 wherein dominant negative mutant of procaspase-9 inhibited paraptosis. Procaspase-9 expression induced both apoptosis and paraptosis (Sperandio *et al.*, 2004). Paraptosis lacks many of the molecular and biochemical characteristics of apoptosis. Paraptosis and apoptosis represent two separate programs of cell death that are induced *via* distinct molecular pathways, but may be induced simultaneously by a single insult or agent. One feature distinguishing paraptotic cell death from apoptotic cell death is that paraptotsis is not affected by broad caspase inhibitor. In particular, apoptosis is inhibited by caspase inhibitors whereas paraptosis is resistant to such inhibitors. Involvement of procaspase-9 in paraptosis is independent of its proteolytic activity in the apoptotic pathway as evidenced by the resistance of paraptosis to Apaf-1. However, *D. discoideum* paraptosis may not be dependent even on procaspase function as this organism lacks caspases. Thus our results point out that paraptotic pathway could be further divided into procaspase-9 dependent and procaspase-9 independent types.

However, PARP inhibition had only marginal protective effects on the events of necrotic cell death. This suggests that at higher doses other mechanisms operate in addition to PARP and AIF to bring about the demise of the stressed cell.

3.4. References

Aboussekhra, A. and Wood, R. D. (1994) Repair of UV-damaged DNA by mammalian cells and Saccharomyces cerevisiae, *Curr. Opin. Genet. Dev. 4*, 212-220.

Alvarez-Gonzalez, R. and Althaus, F. R. (1989) Poly(ADP-ribose) catabolism in mammalian cells exposed to DNA-damaging agents, *Mutat. Res. 218*, 67-74.

Arnoult, D., Tatischeff, I., Estaquier, J., Girard, M., Sureau, F., Tissier, J. P., Grodet, A., Dellinger, M., Traincard, F., Kahn, A., Ameisen, J. C., and Petit, P. X. (2001) On the evolutionary conservation of the cell death pathway: mitochondrial release of an apoptosis-inducing factor during Dictyostelium discoideum cell death, *Mol. Biol. Cell 12*, 3016-3030.

Berger, N. A. and Sikorski, G. W. (1980) Nicotinamide stimulates repair of DNA damage in human lymphocytes, *Biochem. Biophys. Res. Commun. 95*, 67-72.

Boorstein, R. J., Hilbert, T. P., Cunningham, R. P., and Teebor, G. W. (1990) Formation and stability of repairable pyrimidine photohydrates in DNA, *Biochemistry 29*, 10455-10460.

Burkle, A. (2000) Poly(ADP-ribosyl)ation, genomic instability, and longevity, *Ann. N. Y. Acad. Sci. 908*, 126-132.

Chopra, M., Dharmarajan, A. M., Meiss, G., and Schrenk, D. (2009) Inhibition of UV-C light-induced apoptosis in liver cells by 2,3,7,8-tetrachlorodibenzo-p-dioxin, *Toxicol. Sci. 111*, 49-63.

Cipriani, G., Rapizzi, E., Vannacci, A., Rizzuto, R., Moroni, F., and Chiarugi, A. (2005) Nuclear poly(ADP-ribose) polymerase-1 rapidly triggers mitochondrial dysfunction, *J. Biol. Chem. 280*, 17227-17234.

Deering, R. A. (1988) DNA repair in Dictyostelium, *Dev. Genet. 9*, 483-493.

Demple, B. and Linn, S. (1982) 5,6-Saturated thymine lesions in DNA: production by ultraviolet light or hydrogen peroxide, *Nucleic Acids Res. 10*, 3781-3789.

Denecker, G., Declercq, W., Geuijen, C. A., Boland, A., Benabdillah, R., van, G. M., Sory, M. P., Vandenabeele, P., and Cornelis, G. R. (2001) Yersinia enterocolitica YopP-induced apoptosis of macrophages involves the apoptotic signaling cascade upstream of bid, *J. Biol. Chem. 276*, 19706-19714.

Endress, H., Freudenberg, N., Fitzke, E., Grahmann, P. R., Hasse, J., and Dieter, P. (1997) Infiltration of lung carcinomas with macrophages of the 27E10-positive phenotype, *Lung Cancer 18*, 35-46.

Friedberg, E. C. (1996) Relationships between DNA repair and transcription, *Annu. Rev. Biochem. 65*, 15-42.

Hong, S. J., Dawson, T. M., and Dawson, V. L. (2004) Nuclear and mitochondrial conversations in cell death: PARP-1 and AIF signaling, *Trends Pharmacol. Sci. 25*, 259-264.

Jacobson, E. L., Giacomoni, P. U., Roberts, M. J., Wondrak, G. T., and Jacobson, M. K. (2001) Optimizing the energy status of skin cells during solar radiation, *J. Photochem. Photobiol. B 63*, 141-147.

McCurry, L. S. and Jacobson, M. K. (1981) Unscheduled synthesis of DNA and poly(ADP-ribose) in human fibroblasts following DNA damage, *J. Supramol. Struct. Cell Biochem. 17*, 87-90.

Modjtahedi, N., Giordanetto, F., Madeo, F., and Kroemer, G. (2006) Apoptosis-inducing factor: vital and lethal, *Trends Cell Biol. 16*, 264-272.

Rouleau, M., Aubin, R. A., and Poirier, G. G. (2004) Poly(ADP-ribosyl)ated chromatin domains: access granted, *J. Cell Sci. 117*, 815-825.

Saeki, M., Kamisaki, Y., and Maeda, S. (2000) Involvement of mitogen-activated protein kinase in peroxynitrite-induced cell death of human neuroblastoma SH-SY5Y cells, *Neurosci. Res. 38*, 213-216.

Sperandio, S., Poksay, K., de, B., I, Lafuente, M. J., Liu, B., Nasir, J., and Bredesen, D. E. (2004) Paraptosis: mediation by MAP kinases and inhibition by AIP-1/Alix, *Cell Death. Differ. 11*, 1066-1075.

Tornaletti, S., Rozek, D., and Pfeifer, G. P. (1993) The distribution of UV photoproducts along the human p53 gene and its relation to mutations in skin cancer, *Oncogene 8*, 2051-2057.

Vodenicharov, M. D., Ghodgaonkar, M. M., Halappanavar, S. S., Shah, R. G., and Shah, G. M. (2005) Mechanism of early biphasic activation of poly(ADP-ribose) polymerase-1 in response to ultraviolet B radiation, *J. Cell Sci. 118*, 589-599.

Zamzami, N., Marchetti, P., Castedo, M., Zanin, C., Vayssiere, J. L., Petit, P. X., and Kroemer, G. (1995) Reduction in mitochondrial potential constitutes an early irreversible step of programmed lymphocyte death in vivo, *J. Exp. Med. 181*, 1661-1672.

Zhang, J., Lambropoulos, P., and Tang, X. (1994) Radiation amplification near an autoionizing state: A model in atomic Ca, *Phys. Rev. A 50*, 1935-1938.

Zhang, J. S., Nakatsugawa, S., Ishii, Y., Ju, G. Z., and Liu, S. Z. (1994) Experimental radiotherapy and metastasis of human lung cancer xenografts in nude mice, *Chin Med. J. (Engl.) 107*, 491-495.

Zong, W. X., Ditsworth, D., Bauer, D. E., Wang, Z. Q., and Thompson, C. B. (2004) Alkylating DNA damage stimulates a regulated form of necrotic cell death, *Genes Dev. 18*, 1272-1282.